Pharm Res (2015) 32:2038–2050
DOI 10.1007/s11095-014-1597-7

RESEARCH PAPER

Exploring Advantages/Disadvantages and Improvements in Overcoming Gene Delivery Barriers of Amino Acid Modified Trimethylated Chitosan

Hao Zheng • Cui Tang • Chunhua Yin

Received: 29 August 2014 / Accepted: 5 December 2014 / Published online: 23 December 2014

ABSTRACT

Purpose Present study aimed at exploring advantages/disadvantages of amino acid modified trimethylated chitosan in conquering multiple gene delivery obstacles and thus providing comprehensive understandings for improved transfection efficiency.

Methods Arginine, cysteine, and histidine modified trimethyl chitosan were synthesized and employed to self-assemble with plasmid DNA (pDNA) to form nanocomplexes, namely TRNC, TCNC, and THNC, respectively. They were assessed by structural stability, cellular uptake, endosomal escape, release behavior, nuclear localization, and *in vitro* and *in vivo* transfection efficiencies. Besides, sodium tripolyphosphate (TPP) was added into TRNC to compromise certain disadvantageous attributes for pDNA delivery.

Results Optimal endosomal escape ability failed to bring in satisfactory transfection efficiency of THNC due to drawbacks in structural stability, cellular uptake, pDNA liberation, and nuclear distribution. TCNC evoked the most potent gene expression owing to multiple advantages including sufficient stability, preferable uptake, efficient pDNA release, and high nucleic accumulation. Undesirable stability and insufficient pDNA release adversely affected TRNC-mediated gene transfer. However, incorporation of TPP could improve such disadvantages and consequently resulted in enhanced transfection efficiencies.

Conclusions Coordination of multiple contributing effects to conquer all delivery obstacles was necessitated for improved transfection efficiency, which would provide insights into rational design of gene delivery vehicles.

KEY WORDS amino acid modification · gene delivery · nanocomplexes · transfection efficiency

ABBREVIATIONS

ANOVA	Analysis of variance
CLSM	Confocal laser scanning microscopy
CTB	Cholera toxin subunit B
DLS	Dynamic light scattering
DMEM	Dulbecco's modified Eagle's medium
EDC	1-ethyl-3-(3-dimethylaminopropyl) carbodiimide hydrochloride
FBS	Fetal bovine serum
FITC	Fluorescein isothiocyanate
GSH	Glutathione
NC	Nanocomplexes
NHS	*N*-hydroxysuccinimide
pDNA	Plasmid DNA
SEM	Scanning electron microscopy
TR	TMC-Arginine
TRNC	TR/pDNA nanocomplexes
TRNC2	TR/TPP/pDNA nanocomplexes
TC	TMC-Cysteine
TCNC	TC/pDNA nanocomplexes
TH	TMC-Histidine
THNC	TH/pDNA nanocmplexes
TMC	Trimethyl chitosan
TNC	TMC/pDNA nanocomplexes
TPP	Sodium tripolyphosphate

INTRODUCTION

The potent gene transfection efficiency evoked by viral vectors comes at the cost of safety concerns such as carcinogenicity, immunogenicity, and inflammation, thereby severely restricting their *in vivo* applications (1). Comparatively, cationic

Electronic supplementary material The online version of this article (doi:10.1007/s11095-014-1597-7) contains supplementary material, which is available to authorized users.

H. Zheng • C. Tang (✉) • C. Yin
State Key Laboratory of Genetic Engineering
Department of Pharmaceutical Sciences, School of Life Sciences
Fudan University, Shanghai 200433, China
e-mail: tangcui@fudan.edu.cn

polymer-based systems as non-viral vectors possess desirable safety profiles (2). Nonetheless, they suffer from unsatisfactory transfection efficiencies owing to failure in addressing multiple obstacles associated with the gene delivery, including undesirable extracellular stability, poor cellular internalization, endosomal entrapment, low intracellular dissociation, and ineffective nuclear navigation. Introduction of amino acid moieties has been exploited to improve gene delivery performance in various polymeric systems by integrating distinct functionalities to overcome aforementioned barriers (3). Arginine conjugation has been applied in PAMAM (4), polypropylenimine (5), poly (disulfide amine) (6), and trimethyl chitosan (TMC) (7), aiming at bio-mimicking arginine-rich cell penetrating peptides and therefore improving cellular internalization (8). Modification with histidine bearing imidazole ring was commonly supposed to suppress unwanted degradation through facilitating the escape from endo-lysosomal compartments via proton-sponge effect (9–11). Thiolated polymers have been demonstrated to favor gene transfection through uptake-facilitating and release-favoring mechanisms (12–14) and cysteine substitution has been accordingly developed (15).

Collectively, due to their specific functionalities, distinct amino acid modifications would be intended to address disparate challenges to enhance gene delivery performance of polymeric vectors. However, when it comes to the design of delivery vehicles, only overcoming certain obstacles can not meet all the requirements for improving transfection efficiencies. Considering the sophisticated transfection process would be affected by serial interrelated delivery barriers, it seems particularly important to coordinate various functionalities of polymeric vehicles for addressing all delivery obstacles and thus enhancing their transfection efficiencies. Nevertheless, to the best of our knowledge, little attention has been devoted to comprehensively exploring the whole gene delivery process of various amino acid modified polymeric vectors, especially focusing on their advantageous and disadvantageous delivery attributes to elucidate a promising strategy for the improved transfection efficiencies of polymer-based gene delivery systems.

Based on the abovementioned understandings, TMC-arginine (TR), TMC-cysteine (TC), and TMC-histidine (TH) as polymeric vectors were synthesized via carbodiimide-mediated chemistry in this study with the intention of probing their advantageous and disadvantageous characteristics responsible for gene delivery, thereby providing a solution to their low gene transfection efficiencies. Nanocomplexes (NC) were prepared via self-assembly of TR, TC, and TH with plasmid DNA (pDNA). Their detailed characteristics including pDNA condensation and protection, structural stability, cellular uptake, endosomal escape, release behavior, and nuclear localization were investigated. The *in vitro* and *in vivo* transfection efficiencies were monitored as well. Finally, based on above results, sodium tripolyphosphate (TPP) was added into TRNC to compromise their certain disadvantageous attributes, thus enhancing gene transfection efficiencies.

MATERIALS AND METHODS

Materials and Animals

Chitosan (deacetylation degree of 85% and molecular weight (Mw) of 100 kDa) was obtained from Golden-shell Biochemical Co., Ltd. (Zhejiang, China). L-arginine hydrochloride, cysteine, Boc-histidine, 1-ethyl-3-(3-dimethylaminopropyl) carbodiimide hydrochloride (EDC), N-hydroxysuccinimide (NHS), glutathione (GSH), fluorescein isothiocyanate (FITC), chloroquine, bafilomycin A1, nocodazole, and Hoechst 33258 were from Sigma (St. Louis, MO, USA). DNase I was purchased from Worthington (Lakewood, NJ, USA). Plasmid DNA (pDNA) encoding Enhanced Green Fluorescent Protein (pEGFP) was amplified in *E. coli* and purified by an EndoFree Maxi Plasmid Kit (TianGen, Beijing, China).

HEK 293 cells (human embryonic kidney cells) were purchased from the American Type Culture Collection (ATCC, Rockville, MD, USA) and cultured in Dulbecco's modified Eagle's medium (DMEM, Grand Island, NY, USA) supplemented with 10% fetal bovine serum (FBS).

Kunming mice (6 weeks, 18–22 g) were obtained from Slaccas Experimental Animals Co., Ltd. (Shanghai, China) and the investigation protocol was reviewed and approved by the Institutional Animal Care and Use Committee, Fudan University, China.

Synthesis and Characterization of TMC, TR, TC, and TH

TMC was obtained by methylation of chitosan with CH_3I according to the protocol of Kean *et al.* (16). Arginine and cysteine were respectively conjugated to the backbone of TMC via the formation of amide bond as previously described to obtain TR and TC (17,18). As for TH, the carboxyl groups of Boc-histidine were activated in HCl solution (pH 4.8) with EDC and NHS (EDC/NHS: Boc-histidine = 3:1 (m/m)) as catalysts for 2 h, followed by the addition of TMC solution (TMC: Boc-histidine = 2:1 (w/w)) and stirring at room temperature for 24 h (19). HCl solution was subsequently used to detach the Boc group (19). The resultant TR and TH were dialyzed against water while TC was purified by dialysis against HCl solution (pH 5.0). All of the cationic polymers were lyophilized. The characterization of chitosan was performed by ^1H NMR in 1% DCl (w/v) while those of TMC, TR, TC and TH were determined in D_2O on an AVANCE DMX 500 NMR spectrometer (Bruker,

Germany). The trimethylation degrees of polymers were calculated by comparing the peak area of trimethyl protons with those of acetyl protons. The grafting ratios of arginine, cysteine, and histidine were determined through Sakaguchi reaction, Ellman's method, and ninhydrin test, respectively, and calculated as the percentage of all sugar rings [20–22]. Non-trimethylation degree was then calculated as subtracting trimethylation degree and amino acid grafting degree from deacetylation degree. The viscometer was used to determine the viscosity average molecular weight of polymers.

Buffering Capacity and Membrane Disruptive Activity of Cationic Polymers

Acid–base titration was employed to assess the relative buffering capacity of polymers. In brief, polymers were dissolved in water at the concentration of 0.2 mg/mL. The pH value of polymer solution was initially adjusted to around 10.0 with 0.1 M NaOH and titrated with 0.1 M HCl. The pH value was recorded with a pH meter.

The cellular uptake of membrane-impermeable FITC was used to assess the membrane disruptive activity of cationic polymers (23). HEK 293 cells were allowed to grow at 37°C for 24 h. Following change to serum-free DMEM, cationic polymers and FITC were added at the concentration of 2 and 1 mg/mL, respectively. After 2-h incubation, cells were washed with cold phosphate buffered saline (PBS) for three times and lysed with RIPA lysis buffer. The lysate was quantified for FITC content on a microplate reader (Thermofisher, USA) (λ_{ex}=488, λ_{em}=519 nm) and protein content by Lowry method (18). Cells treated with FITC alone served as a negative control.

Preparation, Characterization, and Stability of NC

Cationic polymers were dissolved in water at the concentration of 2 mg/mL and adjusted to pH 6.0 for NC preparation. pDNA was also dissolved in water (pH 6.0) at the concentration of 0.2 mg/mL. An equal volume of polymers and pDNA were mixed under vortex to form NC via spontaneously occurred self-assembly process. The N/P ratios for TNC, TRNC, TCNC, and THNC were 15, 15, 11, and 11, respectively. TMC/pDNA NC (TNC), TR/pDNA NC (TRNC), TC/pDNA NC (TCNC), and TH/pDNA NC (THNC) were incubated at 37°C for 30 min before use. For scanning electron microscopy (SEM) observation of NC morphology, NC were prepared as described above and dropped on the silica surface. After covered by thin-layer of gold, SEM observation was conducted (Vega TS5136, Tescan, Czech).

Particle sizes and Zeta potentials of freshly prepared NC were determined by dynamic light scattering (DLS) with a Zetasizer Nano (Malvern, Worcestershire, UK). To examine the stability, DLS measurements were conducted after NC were diluted up to 50 folds by FBS-free DMEM or 250 folds by PBS (0.2 M, pH 7.4) to mimic the *in vitro* transfection condition and *in vivo* environment, respectively.

Gel retardation assay was employed to evaluate the condensation capacity of polymers towards pDNA. To qualitatively test the protection effect of pDNA against enzymatic degradation, agarose gel electrophoresis was performed following incubation of NC with DNase I (5 U) for 30 min and liberation of pDNA by heparin sodium (10 mg/mL). For quantification analysis, variation in the absorbance at 260 nm ($OD_{260\ nm}$) was continuously monitored after co-incubation of NC and DNase I in the duration of 1-h.

Cellular Uptake

To allow the assessment of uptake of NC, FITC-pDNA was synthesized as previously described (24). NC containing FITC-pDNA were incubated with HEK 293 cells at 37°C for 4 h. Afterwards, cells were washed with cold PBS (0.2 M, pH 7.4) for three times to remove membrane-adsorptive NC and lysed with SDS (0.5% (w/v), pH 8.0). The lysate was quantified for pDNA content by fluorospectrophotometry (λ_{ex}=488, λ_{em}=519 nm) and protein content by Lowry method. Uptake levels were expressed as the amount of FITC-pDNA associated with 1 mg of cellular protein.

To probe into the underlying mechanisms involved in NC endocytosis, we performed uptake experiments in the presence of genistein (200 μg/mL) or chlorpromazine (10 μg/mL). Results were expressed as the percentage of uptake levels as compared with control groups without inhibitor treatment.

Subcellular Distribution

To explore the intracellular distribution of pDNA, NC containing FITC-pDNA were incubated with HEK 293 cells for 4 h prior to cells collection. After washing with cold PBS (0.2 M, pH 7.4), the cell pellet was suspended in TM-2 buffer (10 mM Tris–HCl, 2 mM $MgCl_2$, 0.5 mM PMSF; pH 7.4) and incubated at room temperature and in ice bath for 5 and 1 min, respectively. Following lysing in ice bath by TritonX-100, the lysate was centrifugated at 800 rpm for 10 min to isolate the nuclei. The supernatant proceeded to be centrifugated at 12,000 rpm for 15 min. Subsequently, sucrose density gradient centrifugation was employed to separate mitochondria from endo-lysosome in the precipitation and the supernatant was directly used to quantify the pDNA content in the cytoplasm. The subcellular fraction was calculated as the percentage of pDNA internalized.

For the further visualization of intracellular distribution of pDNA, CLSM observation was conducted after incubation with NC containing FITC-pDNA for 2 h. Nuclei and endo-lysosomal compartments were stained with Hoechst 33258 (10 mg/mL) and Lysotracker Red (100 nM), respectively.

pDNA Release Profiles

FITC-pDNA loaded TNC, TRNC, TCNC, and THNC were incubated at 100 rpm and 37°C in PBS (0.2 M, pH 7.4) containing 0 mM, 4.5 μM, and 10 mM GSH. At pre-determined time intervals, the suspension was centrifugated at 13,300 rpm for 30 min, and the supernatant was withdrawn to quantify the pDNA content ($\lambda_{ex}=488$, $\lambda_{em}=519$ nm). An equal volume of release medium was replenished before further incubation.

MTT Assay

MTT assay was used to analyze the cell viability following the treatment of disparate polymers and NC at various concentrations. Briefly, HEK 293 cells were seeded onto 96-well plate at the density of 1×10^4 cells per well and cultured for 24 h before the addition of distinct polymers at the concentrations of 0.01, 0.05, 0.1, 0.2, 0.4, 0.8, 1, and 2 mg/mL, respectively. As for the NC, they were dosed at the concentrations of 2, 4, 6, 8, and 10 μg pDNA/mL, respectively. After incubation for 96 h, the medium was replaced by fresh DMEM, followed by the addition of MTT solution (5 mg/mL dissolved in PBS, 20 μL per well). Following 3-h incubation, the supernatant was discarded, DMSO was added to dissolve the formazan crystal and the absorbance at 570 nm was measured. Results were expressed as the relative cell viability as compared with the control group that was treated with PBS (0.2 M, pH 7.4).

In Vitro Gene Transfection

HEK 293 cells were seeded onto 24-well plate at the density of 4×10^4 cells per well and incubated for 24 h. NC containing 2 μg of pDNA were incubated with cells for 24, 48, 72, and 96 h, followed by sequential treatment of trypsinization, washing, and resuspending in ice-cold PBS (0.2 M, pH 7.4). Cell suspension was then subjected to the analysis of green fluorescence protein (GFP)-positive percentage by a flow cytometry (FACScan, BD, USA). For the qualitative visualization, transfected cells at 48 h were observed with an IX71 fluorescence microscopy (Olympus, Japan).

For further validation of the involvement of the endo-lysosomal pathways and exploration of underlying mechanisms of endosomal escape, cells were pre-incubated with chloroquine (100 μg/mL), bafilomycin A1 (100 nM), and nocodazole (20 μM) for 30 min before 24-h transfection measurements. Cells treated with NC alone served as a control.

Effect of TPP Addition on Transfection Efficiency of TRNC

NC composed of TA, TPP, and pDNA (TA/TPP/pDNA= 10/0.5/1, w/w/w), termed TRNC2, were prepared as previously described (17). The particle sizes and Zeta potentials before and after PBS and DMEM dilution were measured by DLS. The cellular uptake, pDNA release, subcellular distribution, and *in vitro* transfection efficiencies were determined as abovementioned methods.

Intramuscular Gene Expression

Mice were randomly assigned to 8 groups and intramuscularly injected of saline, naked pDNA, PEI/pDNA NC (Mw of PEI was 25 kDa, N/P ratio of NC was 10), TNC, TRNC, TCNC, THNC, and TRNC2 at the pDNA dosage of 10 μg per mouse ($n=4$). Three days later, posterior tibialis muscular tissues in each group were harvested and homogenized with RIPA buffer. The lysate was centrifugated at 12,000 rpm for 15 min, and pDNA and protein contents in the supernatant were determined by fluorometry ($\lambda_{ex}=488$, $\lambda_{em}=519$ nm) and Lowry method, respectively. The results were denoted as fluorescence intensity associated with 1 mg protein.

Statistically Analysis

All data were expressed as the mean ± standard deviation (mean ± SD). The data were representative of triplicate measurements of each point unless otherwise specified. One-Way Analysis of Variance (ANOVA) with Tukey post hoc test (SPSS, software, version 12.0, SPSS Inc) was employed to make statistical comparison. Differences were judged to be statistically significant at $P<0.05$.

RESULTS

Synthesis and Characterization of TMC, TR, TC, and TH

Chitosan was firstly methylated by CH_3I to obtain TMC with quaternization degree of roughly 30% as calculated by ^1H NMR (Fig. 1 and Table I) (25). The amine groups of TMC were then linked with the carboxyl groups of arginine, cysteine, and histidine via amide bonds to achieve TR, TC, and TH, respectively. The peak at 1.82 ppm in the spectrum of chitosan was assigned to the protons of acetyl groups while one at 3.35 ppm in the ^1H NMR spectrum of TMC belonged to the protons of quaternized methyl groups. Peaks at 2.58, 2.88, and 8.33 ppm in TR, TC, and TH were corresponded to the alkyl protons of arginine, methylene protons of cysteine, and

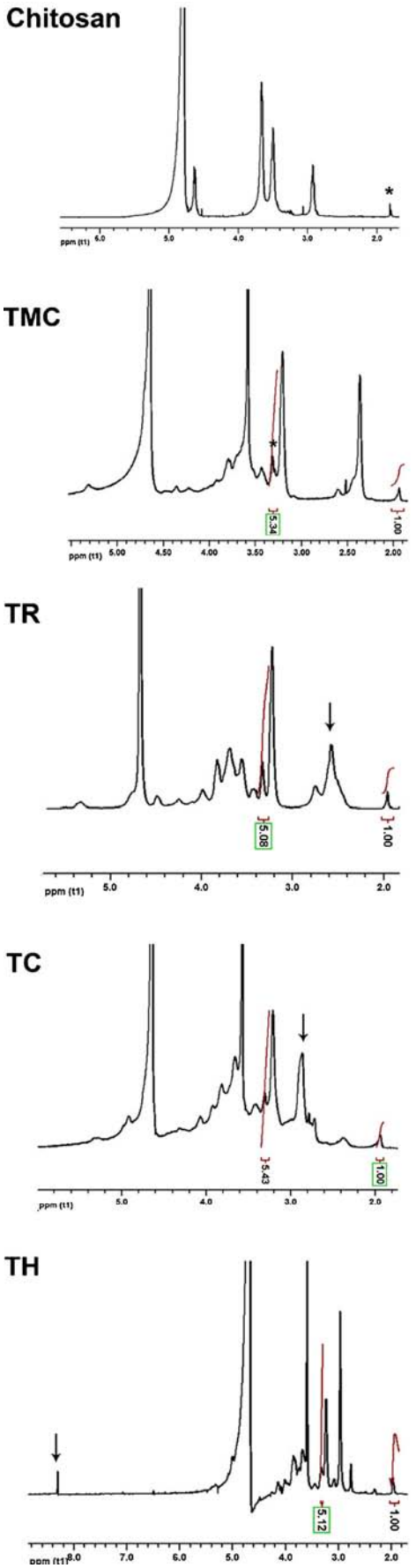

◀ **Fig. 1** ^{1}H NMR spectra of chitosan, TMC, TA, TC, and TH. Peak at 1.82 ppm in the spectrum of chitosan belonged to the protons of acetyl groups (*asterisk*). A peak at 3.35 ppm was assigned to the protons of trimethyl groups (*asterisk*) while ones at 2.58, 2.88, and 8.33 ppm in TA, TC, and TH were corresponded to the alkyl protons of arginine, methylene protons of cysteine, and imidazole protons of hisitidine, respectively (*arrows*).

imidazole protons of hisitidine, respectively, confirming their successful conjugation to TMC (17,19,25–27). The grafting ratios of arginine and histidine were determined as 13.3 ± 0.04 and 12.1 ± 0.4%, respectively (Table I). The free sulphydryl and disulfide bond contents in TC were 145.5 ± 5.8 and 127.6 ± 7.1 μmol/g, respectively, meaning that the grafting ratio of cysteine was 14.3 ± 0.3% (Table I). Besides, amino acid modification exerted negligible influence on the molecular weight of polymers (Table I).

Buffering Capacity and Membrane Disruptive Activity of Cationic Polymers

As displayed in Fig. 2a, TMC, TR, and TC showed similarly moderate buffering effect. In comparison, TH exhibited a smoother titration curve arising from stronger tolerance of hydroxyl groups, indicating its considerable buffering capacity.

As depicted in Fig. 2b, uptake levels of hydrophobic and membrane-impermeable FITC were minimal in the presence of TMC, TC, and TH, but experienced a 6-fold elevation following co-incubation with TR.

Preparation, Characterization, and Stability of NC

Positively charged TMC, TR, TC, and TH could spontaneously interact with negatively charged pDNA via electrostatic attraction to form NC with spherical/subspherical shape as revealed by SEM images (Fig. 3a). The particle sizes of NC composed of distinct cationic polymers ranged from 115 to 150 nm while their Zeta potentials were 22–32 mV (Table II). Restricted migration of pDNA as revealed by gel retardation assay indicated potent pDNA condensation capacity of all cationic polymers in the experimental condition (Fig. 3b).

Table I The Characterizations of Polymers

Sample	Trimethylation degrees (%)	Non-trimethylation degrees (%)	Amino acid modification degrees (%)	Molecular weight (kDa)
TMC	26.7	58.3	–	128.1
TR	25.4	46.3	13.3 ± 0.04	134.7
TC	27.2	45.6	12.1 ± 0.4	139.8
TH	25.6	45.1	14.3 ± 0.3	148.8

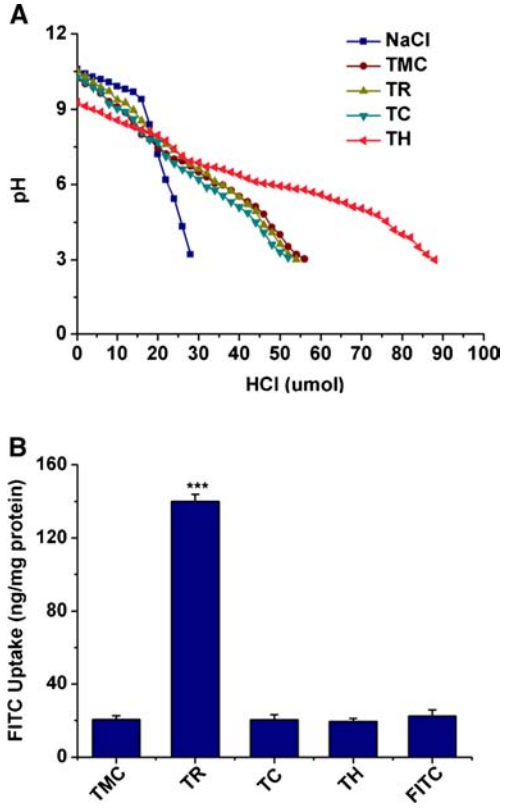

Fig. 2 (**a**) Buffering capacity of polymers as determined by acid–base titration. (**b**) Uptake of FITC with or without polymer treatment. Indicated values were mean ± SD ($n = 3$). * Statistically significant differences observed from FITC (*** $P < 0.001$).

After treatment with DNase I, naked pDNA was completely digested with no bands observed whereas NC provided notable protection with clear pDNA bands (Fig. 3c). A dynamic increase in OD $_{260\ nm}$ was monitored for further quantitative assessment of the protection capacity of distinct polymers. As illustrated in Fig. 3d, naked pDNA experienced rapid degradation as illustrated by marked OD $_{260\ nm}$ elevation. By contrast, polymers could partially suppress such elevation wherein TA and TC outperformed TMC and TH. PBS and DMEM dilution gave rise to elevated particle sizes and decreased Zeta potential of TNC, TRNC, and THNC whereas exerted lessinfluence on TCNC (Table II), suggesting the optimal stability of TCNC.

Cellular Uptake

Cellular uptake amount of distinct NC were depicted in Fig. 4a. As compared with native TNC, histidine modification exerted inappreciable influence on the uptake efficiencies of NC whereas arginine and cysteine conjugation both markedly promoted NC internalization. Additionally, TRNC and TCNC possessed similar uptake levels.

Endocytic inhibitors were used to investigate the detailed uptake mechanisms of NC. As shown in Fig. 4b, prominent depression in the uptake amount of all NC after chlorpromazine treatment suggested that clathrin-mediated endocytosis was mainly responsible for their internalization (28). Nevertheless, pre-incubation with genistein merely yielded a depression of uptake level in TNC, indicating that only TNC was internalized via caveolae-dependent pathway (28).

Subcellular Distribution

Figure 4c quantitatively depicted the subcellular distribution of pDNA in HEK 293 cells. Grafting of amino acids suppressed the endo-lysosomal entrapment and improved the

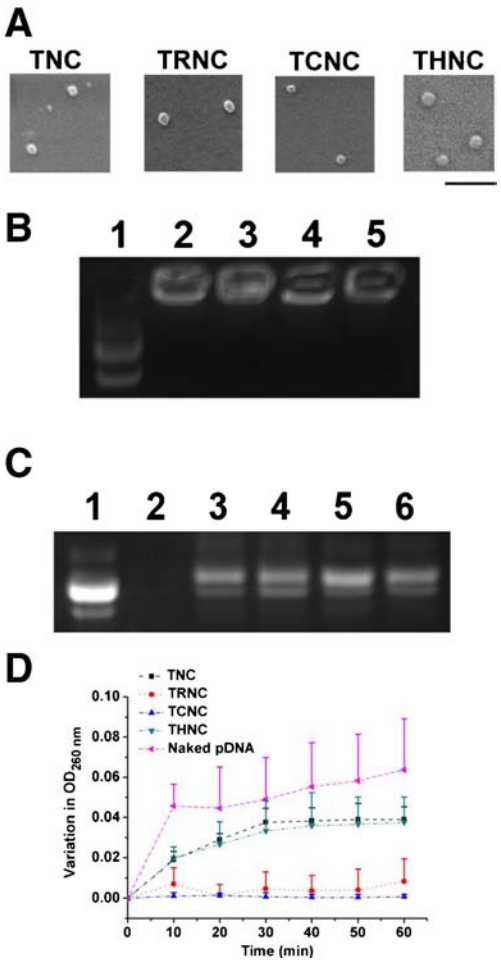

Fig. 3 (**a**) Typical SEM images of NC. *Bar* represented as 1 μm. (**b**) Qualitative analysis of association efficiencies of various NC towards pDNA by gel retardation assay. Lane 1–5 represented naked pDNA, TNC, TRNC, TCNC, and THNC, respectively. (**c**) pDNA integrity post DNase I treatment as demonstrated by agarose gel electrophoresis. Lane 1 represented naked pDNA and lane 2–6 represented naked pDNA, TNC, TRNC, TCNC, and THNC incubated with DNase I, respectively. (**d**) pDNA protection effect as determined by the elevation in OD $_{260\ nm}$. Indicated values were mean ± SD ($n = 3$).

Table II Particle Sizes and Zeta Potentials of NC in Water, DMEM, and PBS. Indicated Values were Mean ± SD ($n = 3$)

Sample	Water		Dilution by 0.2 M PBS at 250 folds		Dilution by DMEM at 50 folds	
	Particle size (nm)[a]	Zeta potential (mV)	Particle size (nm)[a]	Zeta potential (mV)	Particle size (nm)[a]	Zeta potential (mV)
TNC	120.0 ± 1.3 (0.271)	31.6 ± 2.4	305.9 ± 51.3 (0.279)***	16.9 ± 1.1***	237.2 ± 17.7 (0.192) ***	15.4 ± 1.9***
TRNC	147.3 ± 3.6 (0.267)	29.4 ± 2.2	322.4 ± 86.9 (0.273) ***	21.6 ± 3.4***	219.9 ± 17.8 (0.228) ***	20.5 ± 1.0***
TCNC	115.8 ± 2.5 (0.238)	29.3 ± 0.6	131.5 ± 0.6 (0.237) ***	23.4 ± 1.9***	127.1 ± 1.4 (0.263) ***	24.9 ± 1.5***
THNC	150.9 ± 1.5 (0.271)	22.0 ± 0.9	375.3 ± 20.3 (0.369) ***	16.0 ± 0.7***	214.9 ± 5.1 (0.333) ***	19.6 ± 0.7***

[a] Values in parentheses represented the polydispersity index (P.I.)

* Statistically significant differences observed from particle size or Zeta potential that were determined in water (*** $P < 0.001$)

nuclear distribution of pDNA. Specially, THNC possessed the lowest endo-lysosomal accumulation of pDNA while TRNC and TCNC shared similar patterns of nuclear distribution. In addition, CLSM observation further collaborated that all NC were co-localized with Lysotracker Red-stained endo-lysosomal compartments (Fig. 4d).

pDNA Release Profiles

The release behaviors of NC in distinct media were revealed in Fig. 5a–c. The pDNA release profiles of TNC, TRNC, and THNC remained almost the same under various conditions, wherein pDNA release from TRNC and THNC was faster than that from TNC. The pDNA release profiles of TCNC

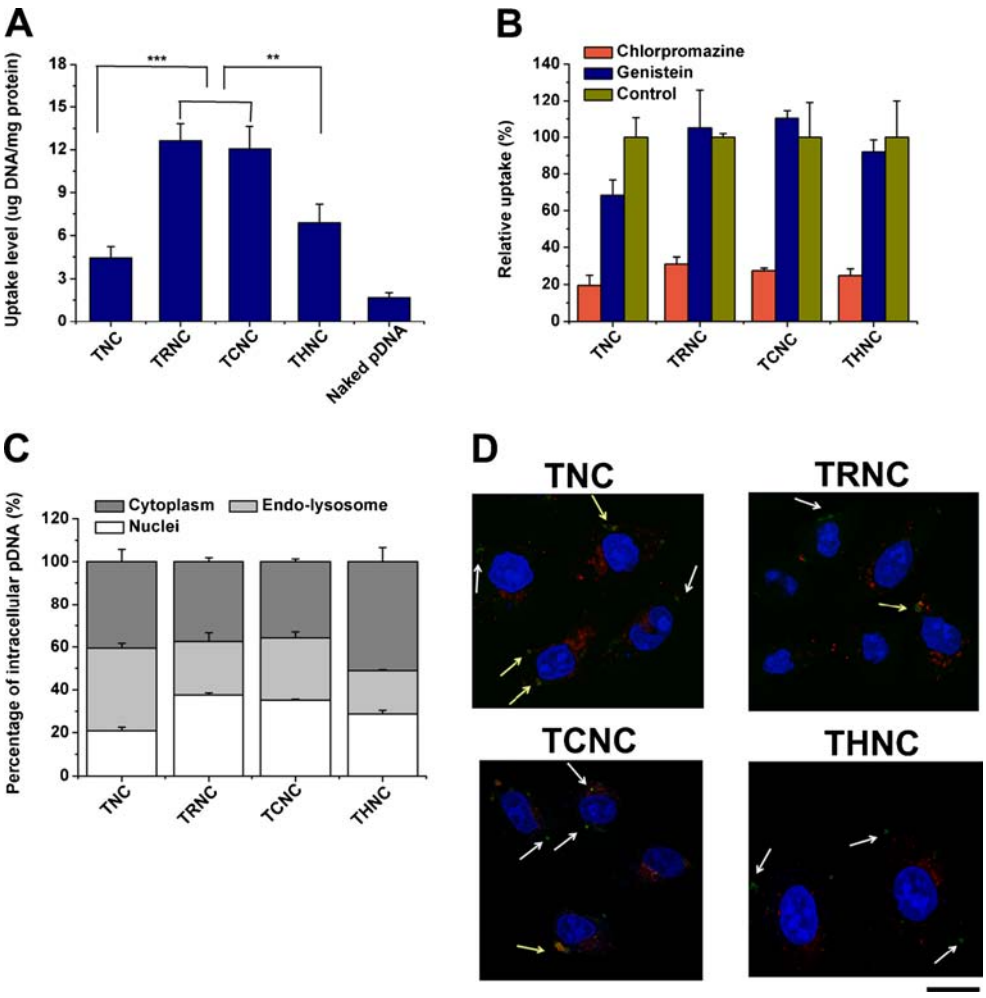

Fig. 4 (**a**) Cellular uptake levels of different NC following incubation with HEK 293 cells for 4 h at 37°C. Indicated values were mean ± SD ($n = 3$). * Statistically significant differences observed from TRNC and TCNC (** $P < 0.01$, *** $P < 0.001$). (**b**) Relative uptake percentages after the treatment of various endocytic inhibitors. Indicated values were mean ± SD ($n = 3$). * Statistically significant differences observed from control (* $P < 0.05$, *** $P < 0.001$). (**c**) pDNA distribution fractions in the nuclei, endo-lysosomal compartments, and cytoplasm of HEK 293 cells after incubation with various NC for 4 h. Indicated values were mean ± SD ($n = 3$). (**d**) CLSM images of HEK 293 cells after treatment of NC (*green*) and subsequent staining of endo-lysosomal compartments (*red*) and nuclei (*blue*) with Lysotracker® Red and Hoechst 33258, respectively. *Arrows* indicated the co-localization of NC and Lysotracker® Red. *Bar* represented as 10 μm.

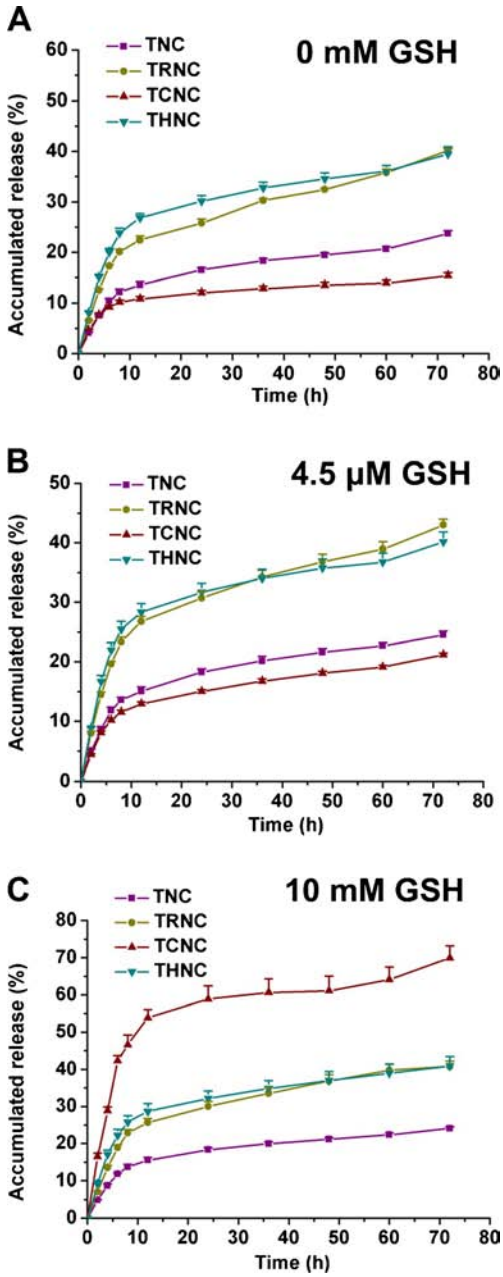

Fig. 5 Release behaviors of distinct NC in PBS (0.2 M, pH 7.4) in the presence of 0 mM (**a**), 4.5 μM (**b**) or 10 mM GSH (**c**). Indicated values were mean ± SD ($n = 3$).

followed a GSH-responsive pattern. Low GSH concentration (extracellular media) induced restricted pDNA release whereas high GSH concentration (intracellular environment) evidently promoted TCNC dissociation. Collectively, NC with amino acids conjugation favored pDNA release in comparison with TNC.

MTT Assay

As indicated in Fig. 6a, all polymers showed inappreciable cytotoxicity even at the concentration of 2 mg/mL, as evidenced by relative cell viabilities all exceeding 80%. NC composed of different polymers also exhibited desirable safety profiles, with cell viabilities above 90% up to the concentration of 10 μg pDNA/mL (Fig. 6b).

In Vitro Gene Transfection

As illustrated in Fig. 6c, arginine modification, cysteine graft, and histidine conjugation all mediated appreciable enhancement in the transfection efficiencies compared to TNC. Moreover, TCNC outperformed the other candidates including Lipofectamine 2000/pDNA complexes. Fluorescence images at 48 h were well accorded with quantitative analyses (Fig. 6d). Additionally, the transfection efficiencies for all NC were increased with the incubation time except for TCNC who reached peak value at 48 h.

Chloroquine, bafilomycin A1, and nocodazole were adopted to explore the underlying endosomal escape mechanisms. As shown in Fig. 6e, dramatic enhancement and appreciable suppression in transfection efficiency induced by chloroquine and bafilomycin A1, respectively, were noted for all NC. Transfection efficiencies of TNC, TCNC, and THNC following nocodazole treatment were almost similar with the control whereas that of TRNC was profoundly increased.

Effect of TPP Addition on Transfection Efficiency of TRNC

Since the abovementioned results demonstrated that TRNC, TCNC, and THNC possessed certain advantages in conquering gene delivery barriers as illustrated in Fig. 7, they presented higher transfection efficiencies compared to TNC. Meanwhile, it was also noted that relatively inferior gene delivery performance of TRNC to TCNC might result from their undesirable stability and delayed dissociation. To compromise such disadvantages, TPP as an ionic crosslinking agent was incorporated into TRNC to form TRNC2. Unlike that of TRNC, particle sizes of TRNC2 remained the initial values after PBS and DMEM dilution, demonstrating their excellent structural stability (Fig. 8a). The uptake level of TRNC2 was 11.9 ± 0.9 μg DNA/mg protein, and the distribution fractions in the nuclei, endosomes, and cytoplasm were determined as 38.2 ± 3.3, 24.3 ± 2.8, and 37.5 ± 3.0%, respectively, all of which were similar with those of TRNC ($P > 0.05$). As demonstrated in Fig. 8b, TPP evidently promoted pDNA dissociation from TRNC2 in all release media in comparison with TRNC. The *in vitro* transfection efficiency of TRNC2 reached the summit at 72 h, which was remarkably higher than that of TRNC at 96 h ($P < 0.05$) (Fig. 8c).

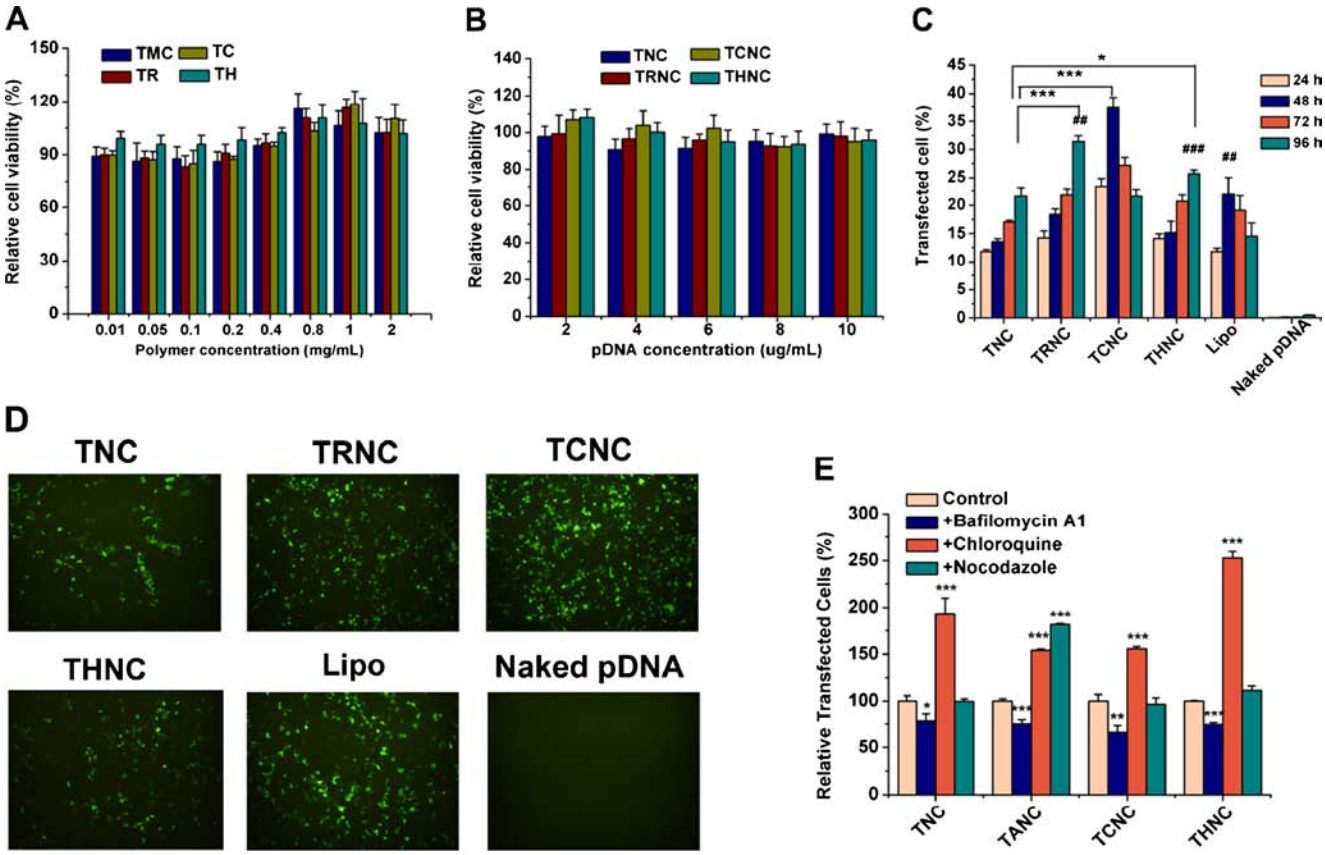

Fig. 6 (**a**) Relative cell viabilities following exposure to different polymers at the concentration of 0.01, 0.05, 0.1, 0.2, 0.4, 0.8, 1, and 2 mg/mL, respectively, for 96 h. Indicated values were mean ± SD ($n = 6$). (**b**) Relative cell viabilities after treatment of disparate NC at the concentrations of 2, 4, 6, 8, and 10 μg pDNA/mL, respectively, for 96 h. Indicated values were mean ± SD ($n = 6$). (**c**) Flow cytometry analyses of GFP-positive percentage of transfected cells with various NC treatment from 24 h to 96 h. Naked pDNA and Lipofectamine 2000/pDNA complexes were denoted as a negative and positive control, respectively. Indicated values were mean ± SD ($n = 3$). * Statistically significant differences observed from TNC at 96 h (* $P < 0.05$, *** $P < 0.001$). $^{\#}$ Statistically significant differences observed from TCNC at 48 h ($^{\#\#}$ $P < 0.01$, $^{\#\#\#}$ $P < 0.001$). (**d**) Representative images of HEK 293 cells that expressed GFP after transfection for 48 h. (**e**) Effects of pre-treatment of chloroquine, bafilomycin A1, and nocodazole on the transfection efficiencies of NC. Indicated values were mean ± SD ($n = 3$). * Statistically significant differences observed from control (* $P < 0.05$, ** $P < 0.01$, *** $P < 0.001$).

Intramuscular Gene Expression

In vivo gene expression mediated by NC was investigated after intramuscular administration. As illustrated in Fig. 9, the GFP expression mediated by amino acid modified derivatives were significantly more potent that native TMC wherein TCNC top-performed. Moreover, TRNC2 was superior to TRNC in terms of *in vivo* gene transfer ability.

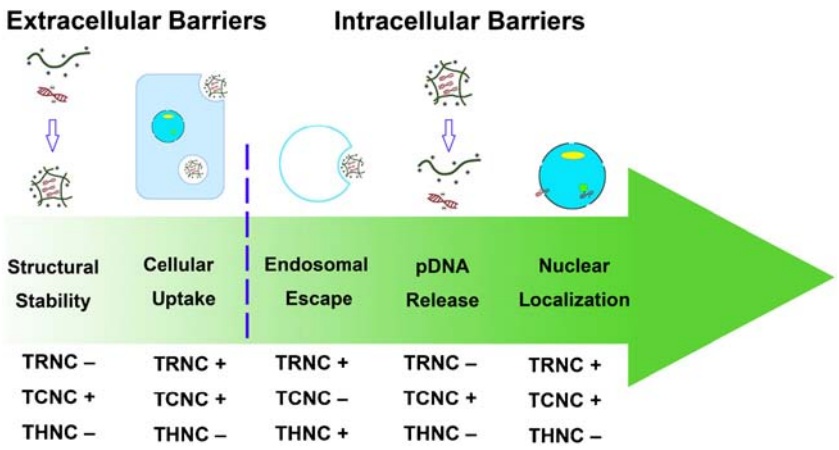

Fig. 7 A schematic image showing the advantages and disadvantages of TRNC, TCNC, and THNC in overcoming certain delivery barriers for efficient transfection.

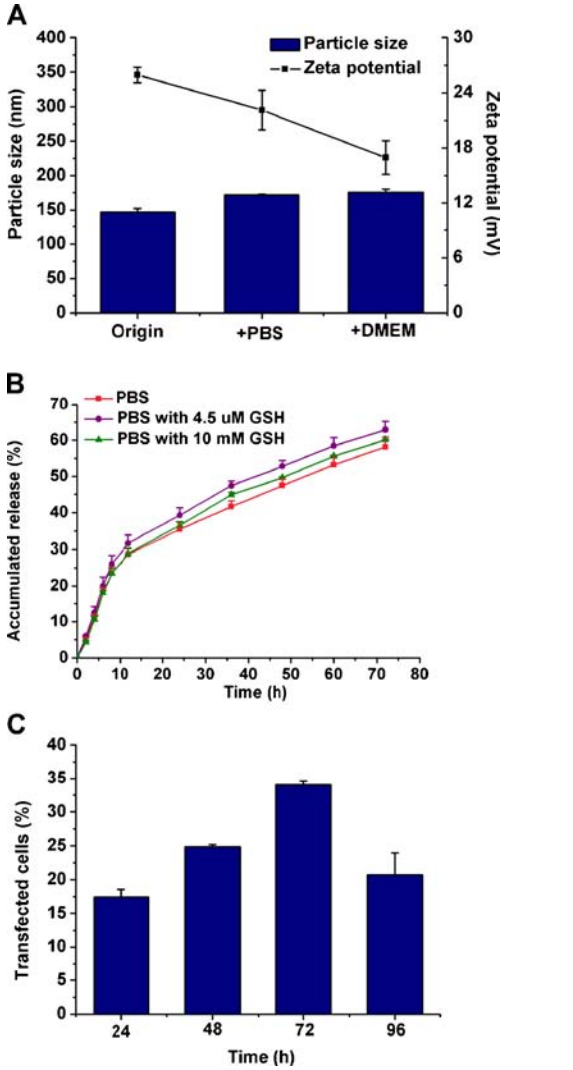

Fig. 8 (**a**) Particle sizes and Zeta potentials of TRNC2 before and after PBS and DMEM dilution. Indicated values were mean ± SD ($n = 3$). (**b**) *In vitro* release profiles of TRNC2 in PBS (0.2 M, pH 7.4) with 0 mM, 4.5 μM, and 10 mM GSH. Indicated values were mean ± SD ($n = 3$). (**c**) *In vitro* transfection efficiencies of TRNC2 on HEK 293 cells from 24 h to 96 h. Indicated values were mean ± SD ($n = 3$).

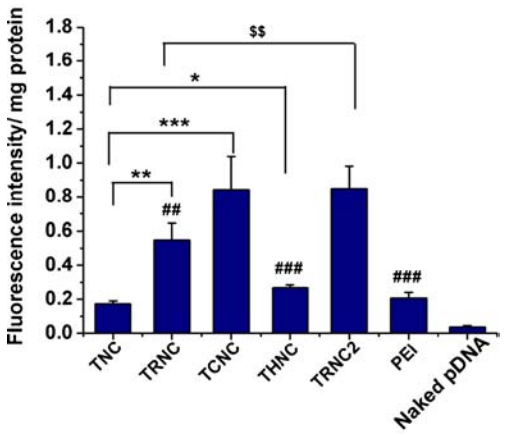

Fig. 9 GFP expression in the muscular tissues 3 days after administration of NC into the posterior tibialis muscles of mice. Naked pDNA and PEI/pDNA complexes were denoted as a negative and positive control, respectively. Indicated values were mean ± SD ($n = 4$). * Statistically significant differences observed from TNC (*$P < 0.05$, ** $P < 0.01$, *** $P < 0.001$). $^{\#}$ Statistically significant differences observed from TCNC ($^{\#\#}$ $P < 0.01$, $^{\#\#\#}$ $P < 0.001$). $^{\$}$ Significant differences between TRNC and TRNC2 ($^{\$\$}$ $P < 0.01$).

DISCUSSION

The gene transfection efficiency of polymeric delivery systems was still required for improvement. Strategies for design of such vehicles called for deliberate considerations on addressing sequential obstacles that lay on the pathway to gene expression. In the current investigation, amino acid modification was employed to ameliorate the gene delivery performance of polymeric vehicles through exploring their whole delivery process to coordinate various functionalities for addressing all of delivery obstacles.

Chitosan has been widely applied as a gene delivery vehicle due to its biocompatibility, biodegradability, and cationic nature. However, one substantial drawback for the application of chitosan lies in its limited solubility under physiological conditions. To this end, trimethylated derivative, namely TMC, was developed. TMC exhibited excellent solubility in wide pH range owing to the highly positive charges of quaternary amine groups. Consequently, in the current system, TMC was employed as the polymer backbone for the synthesis of amino acid conjugated derivatives. TR, TC, and TH, which were obtained from same batch of TMC to eliminate unwanted interferences, were subsequently synthesized via carbodiimide-mediated coupling reaction and their chemical structures were confirmed by ^{1}H NMR (Fig. 1). Self-assembly process spontaneously occurred via the electrostatic interactions between oppositely charged polymers and genetic materials, thus resulting in the compaction of pDNA to form NC (Fig. 3a). Increased particle sizes suggested relatively "loosen" structure of NC after arginine and histidine conjugation (Table II), possibly owing to the occupation of primary amine groups by amide reaction. By contrast, cysteine grafting did not compromise the association affinity, which might be ascribed to the existence of disulfide bridges.

Enzymatic degradation, massive dilution along with ionic components constituted primary extracellular barriers for gene delivery. Prevalent nuclease would render pDNA susceptible to degradation while dilution and ions would cause the structural damage of NC (29). In this study, dilution and ions caused increased particle sizes and decreased Zeta potentials of TNC, TRNC, and THNC due to jeopardized binding force and charge screening effect, respectively (Table II). Comparatively, they exerted slight influence on the particle sizes and Zeta potentials of TCNC owing to stabilization effect of internal disulfide bonds, which contributed to conferring protection against enzymatic degradation (Fig. 3c–d)

(18). Collectively, desirable stability of TCNC would be favorable for gene delivery whereas inferior ones of TRNC and THNC would adversely affect gene transfection.

Desirable safety profiles of different polymers and NC indicated by MTT assay ensured the successful cellular and intracellular processing of all NC (Fig. 6a–b). Internalization, as the premise to initiate gene transfection, was evaluated next. Histidine modification failed to increase the uptake level as compared with TMC, possibly owing to the increased particle sizes in DMEM media and the lack of uptake-facilitating functional groups (Fig. 4a). However, loosened structure did not compromise the uptake efficiency of TRNC and underlying reasons were therefore probed. Despite the well-characterized uptake modes of arginine-rich peptides, there was a lack of investigations concerning the ways that arginine-containing polymer-based NC adopted to enter into targeted cells. Appreciable elevation in uptake levels of membrane-impermeable FITC accompanied with TA treatment implied its active membrane-disruptive activity (Fig. 2b) (30), which could possibly induce a direct penetration into membranes to gain the entrance to cells and correspondingly enhance uptake levels of TRNC. Additionally, TCNC also exhibited improved cellular uptake, owing to their excellent stability under culture medium and binding affinity with cysteine-rich glycoprotein domains in the cell membranes via oxidization of free sulphydryl (Fig. 4a) (18). In sum, promoted uptake of TRNC and TCNC resulting from assorted mechanisms would be beneficial for gene transfection whereas inefficient uptake constituted as another detrimental factor for improving gene delivery efficacy of THNC.

Uptake mechanisms were then investigated due to their close interrelation with intracellular trafficking and ultimate transfection performance (30). Appreciably depressed uptake levels accompanied with chlorpromazine treatment (Fig. 4b) and co-localization with endo-lysosomal compartments as observed by CLSM (Fig. 4d) implied that clathrin-mediated endocytosis was involved in the internalization of NC, which led to their endo-lysosomal entrapment and subsequent degradation. Additionally, augmented transfection efficiencies triggered by chloroquine, an endosomolytic reagent, also indicated that all NC would enter endo-lysosomal compartments once internalized (Fig. 6e) (31,32). Consequently, reduction or avoidance of endosomal entrapment was particularly important for successful gene transfection (33). In the current investigation, arginine, cysteine, and histidine modification escalated endosomal escape efficiencies via disparate mechanisms at varying degrees. Dramatic decrease in transfection efficiencies following treatment with bafilomycin A1 suggested that proton influx-induced osmotic increase was probably responsible for the endosomal escape of all NC (Fig. 6e). Molecules with buffering domains could facilitate endosomal fragmentation of polymeric vectors via proton-sponge effect (34), among which histidine bearing imidazole ring emerged as an appealing candidate. Most desirable buffering capacity of TH among all the polymers as evidenced by acid–base titration experiment (Fig. 2a) led to least endosomal trapping of THNC (Fig. 4c). The endosomal escape efficiencies of TCNC were the lowest among the three candidates, possibly owing to the moderate buffering capacity of primary amines. Despite resemblance in buffering capacity with TC, TA endowed NC better endosomal escape capacities, which was legitimately deduced to correlate with its membrane-disruptive activity. Nocodazole, which prevented the transportation from early endosomes to late endosomes, was employed to validate such presumption (35,36). As expected, it caused the accumulation of TRNC in early endosomes, which facilitated their endosomal escape via membrane penetration mechanisms (37) and then induced the remarkably elevated transfection efficiencies (Fig. 6e).

A previous study had demonstrated that timely dissociation was another paramount component for successful gene transfection (38). As for TCNC, breakable disulfide bonds helped offer sufficient stability in the extracellular media and uncompromised release-favoring mechanisms in the reductive intracellular environment (Fig. 5a–c). Comparatively, relatively tight association with pDNA of TA and TH might delay the NC dissociation in the intracellular media, serving as another contributing factor for their unsatisfactory transfection efficiencies.

Considering that exogenous transgene expression required the nuclear localization of pDNA, enhanced nuclear accumulation would definitely favor transgene expression both *in vitro* and *in vivo*. In comparison with TNC, TRNC, TCNC, and THNC all exhibited promoted nuclear distribution of pDNA due to membrane penetrative capacity, timely dissociation, and better endosomal escape, respectively.

TNC performed ineffectively in terms of NC stability, cellular uptake, endosomal escape, pDNA liberation, and nuclear accumulation, thus resulting in unsatisfactory transfection efficiencies. Conversely, TA, TC, and TH displayed distinct advantages over native TMC by addressing specific dilemmas confronted by gene delivery systems (Fig. 7), thereby bringing in appreciable enhancement of transfection efficiencies both *in vitro* and *in vivo* (Figs. 6c and 9). However, various amino acid modifications brought in discrepant extent of gene expression, allowing us to explore their advantages/disadvantages in the whole transfection process and thereby providing comprehensive understandings for improved transfection efficiencies. THNC displayed most satisfactory feature in terms of endosomal disruption, nevertheless, undesirable structural stability, insufficient uptake amount, delayed pDNA liberation, and relatively disadvantageous pDNA nuclear distribution led to lower transfection efficiencies as compared with TRNC and TCNC, implying that strong endosomal escape ability alone could hardly parallel effective transgene expression. In comparison with THNC, poor stability and

insufficient pDNA release of TRNC were compensated by increment in uptake level, endosomal escape, and nucleic accumulation, therefore leading to improved transfection efficiencies. Despite moderate endosomal escape efficiencies, TCNC still top-performed with regard to GFP expression both *in vitro* and *in vivo* (Figs. 6c and 9), attributing to their excellent physiochemical stability, appealing uptake levels, desirable reducing environment-inductive release mechanisms in combination with preferable nuclear distribution. In addition, the disparity in transfection kinetics of NC might result from varied pDNA release profiles, wherein TRNC and THNC with continuous pDNA release allowed for relatively persistent transfection while TCNC with readily pDNA release were inclined to provoke efficient short-term gene expression (38). Such results suggested that for the design of efficient gene delivery systems, it is highly necessitated to delicately balance and coordinate various effects to conquer all delivery obstacles. As discussed above, inferior gene delivery efficacies of TRNC were mainly attributed to their undesirable stability and delayed pDNA dissociation. Our previous study had demonstrated that the addition of anionic crosslinking agents could improve transfection efficiencies through traversing aforementioned obstructions (17). TPP was therefore employed to surmount the disadvantages of TRNC for enhanced gene expression. TPP incorporation might cause the intramolecular entanglement of TA and competitively interact with TA, resulting in improved NC stability against dilution and ions challenges and promoted intracellular pDNA release, respectively (Fig. 8a–b). Owing to these improvements, TRNC2 exhibited markedly enhanced gene transfection efficiencies as compared to native TRNC ($P<0.05$) (Fig. 8c). Such results substantiated that compromising the disadvantageous delivery attributes of polymeric vectors and meanwhile maintaining their advantageous delivery attributes could further improve their transfection efficiencies.

Unsatisfactory *in vivo* gene transfer efficacy impeded the application of many non-viral delivery systems. In the current investigation, the results of intramuscular transfection correlated well with those obtained in the *in vitro* experiments, where TCNC mediated the most potent GFP expression. Such results were ascribed to their superiorities in overcoming sequential gene delivery barriers, including disulfide bonds-enhanced structural stability, increased uptake arising from disulfide formation with membrane glycoproteins, GSH-responsive pDNA release together with desirable nuclear localization. The higher transfection efficiency of TRNC2 than that of TRNC revealed that the incorporation of TPP in NCs was beneficial to their *in vivo* performance as well, which was associated with promoted pDNA release in combination with strengthened structural stability. In summary, in accordance with *in vitro* analysis, the *in vivo* results also indicated that conquering all gene delivery obstacles would contribute to enhanced gene delivery efficiency.

In a previous investigation, arginine, histidine, and lysine were utilized to modify native chitosan to improve its solubility and transfection efficiency by mimicking the components of viral envelope (39). As compared with unmodified chitosan, amino acids grafted derivatives all exhibited appreciably enhanced transfection efficiency both *in vitro* on HEK 293 cells and *in vivo* after intramuscular injection, which was in accordance with the results of amino acid modified TMC derivatives in this study. In addition, chitosan-based polymers possessed excellent biocompatibility as revealed by cell viability above 95% up to the polymer concentration of 0.2 mg/mL. As for TMC-based derivatives, they all exhibited negligible cytotoxicity even at the concentration of 2 mg/mL (Fig. 6a), demonstrating their preferable safety profiles, which might render TMC and its derivatives as promising platforms for *in vivo* applications. However, in comparison with those based on chitosan, NC composed of TMC and TMC based-derivatives possessed more potent compaction ability towards genetic payloads, evidenced by higher Zeta potentials at lower N/P ratios. This might be ascribed to more fixed positive charges conferred by trimethyl groups. Such higher permanent positive charges of TMC also contributed to the improved solubility at physiological conditions in comparison with chitosan, which presented TMC-based polymers as more desirable candidates for gene delivery.

CONCLUSIONS

Amino acids modification was shown as a feasible way to improve transfection efficiencies of polymeric vectors both *in vitro* and *in vivo* through overcoming distinct gene delivery barriers. Tailoring the species of amino acids allowed us to investigate their advantageous and disadvantageous attributes for gene delivery of polymeric vehicles. TCNC as the optimal candidate for gene delivery might result from their desirable stability, high cellular uptake, GSH-responsive release-favoring mechanism in combination with preferable nuclear distribution. Incorporation of TPP into TRNC could improve their transfection efficiencies through promoting the pDNA release and enhancing the stability of TRNC. Our investigation emphasized on the coordination of multiple contributing effects to conquer all delivery obstacles, which could shed light on the development of efficient gene delivery systems.

ACKNOWLEDGMENTS AND DISCLOSURES

The authors would like to thank for the financial support from the National Natural Science Foundation of China (No. 81172995 and No. 81273460).

REFERENCES

1. Pichon C, Billiet L, Midoux P. Chemical vectors for gene delivery: uptake and intracellular trafficking. Curr Opin Biotech. 2010;21(5): 640–5.
2. Pack DW, Hoffman AS, Pun S, Stayton P. Design and development of polymers for gene delivery. Nat Rev Drug Discov. 2005;4(7):581–93.
3. Casettari L, Vllasaliu D, Lam J. Biomedical applications of amino acid-modified chitosans: a review. Biomaterials. 2012;33(30):7565–83.
4. Choi J, Nam K, Park J, Kim J, Lee J, Park J. Enhanced transfection efficiency of PAMAM dendrimer by surface modification with L-arginine. J Control Release. 2004;99(3):445–56.
5. Kim T, Baek J, Bai C, Park J. Arginine-conjugated polypropylenimine dendrimer as a non-toxic and efficient gene delivery carrier. Biomaterials. 2007;28(11):2061–7.
6. Kim T, Ou M, Lee M, Kim S. Arginine-grafted bioreducible poly (disulfide amine) for gene delivery systems. Biomaterials. 2009;30(4): 658–64.
7. Morris VB, Sharma CP. Folate mediated *in vitro* targeting of depolymerised trimethylated chitosan having arginine functionality. J Colloid Interf Sci. 2010;348(2):360–8.
8. Khalil K, Kogure K, Futaki S, Harashima H. Octaarginine-modified liposomes: enhanced cellular uptake and controlled intracellular trafficking. Int J Pharmaceut. 2008;354(1–2):39–48.
9. Midoux P, Pichon C, Yaouanc J, Jaffres P. Chemical vectors for gene delivery: a current review on polymers, peptides and lipids containing histidine or imidazole as nucleic acids carriers. Brit J Pharmacol. 2009;157(2):166–78.
10. Gu J, Wang X, Jiang X, Chen Y, Chen L, Fang X, *et al.* Self-assembled carboxymethyl poly (L-histidine) coated poly (β-amino ester)/DNA complexes for gene transfection. Biomaterials. 2012;33(2):644–58.
11. Benns J, Choi J, Mahato R, Park J, Kim S. pH-sensitive cationic polymer gene delivery vehicle: N-Ac-poly(L-histidine)-graft-poly(L-lysine) comb shaped polymer. Bioconjug Chem. 2000;11(5):637–45.
12. Schmitz T, Bravo-Osuna I, Vauthier C, Ponchel G, Bernkop-Schnurch A. Development and in vitro evaluation of a thiomer-based nanoparticulate gene delivery system. Biomaterials. 2007;28(3):524–31.
13. Lee D, Zhang W, Shirley S, Kong X, Hellermann G, Lockey R, *et al.* Thiolated chitosan/DNA nanocomplexes exhibit enhanced and sustained gene delivery. Pharm Res. 2007;24(1):157–67.
14. Peng Q, Zhong Z, Zhuo R. Disulfide cross-linked polyethylenimines (PEI) prepared via thiolation of low molecular weight PEI as highly efficient gene vectors. Bioconjug Chem. 2008;19(2):499–506.
15. Lo S, Wang S. An endosomolytic Tat peptide produced by incorporation of histidine and cysteine residues as a nonviral vector for DNA transfection. Biomaterials. 2008;29(15):2408–14.
16. Kean T, Roth S, Thanou M. Trimethylated chitosans as non-viral gene delivery vectors: cytotoxicity and transfection efficiency. J Control Release. 2005;103(3):643–53.
17. Zheng H, Tang C, Yin C. The effect of crosslinking agents on the transfection efficiency, cellular and intracellular processing of DNA/polymer nanocomplexes. Biomaterials. 2013;34(13):3479–88.
18. Zhao X, Yin L, Ding J, Tang C, Gu S, Yin C, *et al.* Thiolated trimethyl chitosan nanocomplexes as gene carriers with high *in vitro* and *in vivo* transfection efficiency. J Control Release. 2010;144(1):46–54.
19. Layek B, Singh J. Amino acid grafted chitosan for high performance gene delivery: comparison of amino acid hydrophobicity on vector and polyplex characteristics. Biomacromolecules. 2013;14(2):485–94.
20. Francis P, Barnett N, Foitzik R, Gange M, Lewis S. Chemiluminescence from the Sakaguchi reaction. Anal Biochem. 2004;329(2):340–1.
21. Han L, Tang C, Yin H. Effect of binding affinity for siRNA on the *in vivo* antitumor efficacy of polyplexes. Biomaterials. 2013;34(21): 5317–27.
22. Sun S, Lin Y, Weng Y, Chen M. Efficiency improvements on ninhydrin method for amino acid quantification. J Food Compos Anal. 2006;19(2–3):112–7.
23. Ter-Avetisyan G, Tuennemann G, Nowak D, Nitschke M, Herrmann A, Drab M, *et al.* Cell entry of arginine-rich peptides is independent of endocytosis. J Biol Chem. 2009;284(6):3370–8.
24. Ishii T, Okahata Y, Sato T. Facile preparation of a fluorescence-labeled plasmid. Chem Lett. 2000;4:386–7.
25. Thanou M, Kotze A, Scharringhausen T, LueBen H, de Boer A, Verhoef J, *et al.* Effect of degree of quaternization of N-trimethyl chitosan chloride for enhanced transport of hydrophilic compounds across intestinal Caco-2 cell monolayers. J Control Release. 2000;64(1–3):15–25.
26. Ding J, He R, Zhou G, Tang C, Yin C. Multilayered mucoadhesive hydrogel films based on thiolated hyaluronic acid and polyvinylalcohol for insulin delivery. Acta Biomater. 2012;8(10): 3643–51.
27. Azari F, Sandros M, Tabrizian M. Self-assembled multifunctional nanoplexes for gene inhibitory therapy. Nanomed-UK. 2011;6(4): 669–80.
28. Khalil IA, Kogure K, Akita H, Harashima H. Uptake pathways and subsequent intracellular trafficking in nonviral gene delivery. Pharmacol Rev. 2006;58(1):32–45.
29. He C, Yin L, Tang C, Yin C. Multifunctional polymeric nanoparticles for oral delivery of TNF-α siRNA to macrophages. Biomaterials. 2013;34(11):2843–54.
30. Yin L, Song Z, Kim K, Zheng N, Tang H, Lu H, *et al.* Reconfiguring the architectures of cationic helical polypeptides to control non-viral gene delivery. Biomaterials. 2013;34(9):2340–9.
31. Thomas J, Rekha M, Sharma C. Unraveling the intracellular efficacy of dextran-histidine polycation as an efficient nonviral gene delivery system. Mol Pharmaceut. 2012;9(1):121–34.
32. Shigeta K, Kawakami S, Higuchi Y, Okuda T, Yagi H, Yamashita F, *et al.* Novel histidine-conjugated galactosylated cationic liposomes for efficient hepatocyte-selective gene transfer in human hepatoma HepG2 cells. J Control Release. 2007;118(2):262–70.
33. Hu Y, Haynes M, Wang Y, Liu F, Huang L. A highly efficient synthetic vector: nonhydrodynamic delivery of DNA to hepatocyte nuclei *in vivo*. ACS Nano. 2013;7(6):5376–84.
34. Chang K, Higuchi Y, Kawakami S, Yamashita F, Hashida M. Development of lysine-histidine dendron modified chitosan for improving transfection efficiency in HEK 293 cells. J Control Release. 2011;156(2):195–202.
35. Gabrielson N, Lu H, Yin L, Li D, Wang F, Cheng J. Reactive and bioactive cationic α-helical polypeptide template for nonviral gene delivery. Angew Chem Int Edit. 2012;51(5): 1143–7.
36. Gilleron J, Querbes W, Zeigerer A, Borodovsky A, Marscio G, Schubert U, *et al.* Image-based analysis of lipid nanoparticle-mediated siRNA delivery, intracellular trafficking and endosomal escape. Nat Biotechnol. 2013;31(7):638–49.
37. Bayer N, Schober D, Prchla E, Murphy R, Blaas D, Fuchs R. Effect of bafilomycin A1 and nocodazole on endocytic transport in HeLa cells: implications for viral uncoating and infection. J Virol. 1998;72(12):9645–55.
38. Grigsby CL, Leong KW. Balancing protection and release of DNA: tools to address a bottleneck of non-viral gene delivery. J R Soc Interface. 2010;7(1):S67–82.
39. Chang J, Xu X, Li H, Jian Y, Wang G, He B, *et al.* Components simulation of viral envelope via amino acid modified chitosans for efficient nucleic acid delivery: *in vitro* and *in vivo* study [J]. Adv Funct Mater. 2013;23(21):2691–9.